Crystalline Orientation and Adhesion at Polypropylene/Polyamide 6 Interfaces Compatibilized with Syndiotactic Polypropylene−Polyamide 6 Diblock Copolymers

Claire Laurens,[†,§] Raymond Ober,[†] Costantino Creton,[‡] and Liliane Léger*[,†]

Laboratoire de Physique des Fluides Organisés, UMR 7125 CNRS-Collège de France, 11 place Marcelin Berthelot, 75231 Paris Cedex 05, France, and Laboratoire de Physico-Chimie Structurale et Macromoléculaire, UMR 7615 CNRS-ESPCI, 10 rue Vauquelin, 75231 Paris Cedex 05, France

Received January 30, 2004; Revised Manuscript Received June 10, 2004

ABSTRACT: Assemblies of polyamide 6 (PA6) with both syndiotactic and isotactic polypropylene (sPP and iPP) have been investigated in the presence of sPP−PA6 diblock copolymers formed in situ at the interface during annealing. Both iPP/PA6 and sPP/PA6 interfaces were stabilized by the sPP−PA6 copolymers. Crystalline orientations at the interface, characterized by X-ray diffraction using thin film assemblies, demonstrated an epitaxial crystallization of sPP on PA6, with a degree of orientation of the sPP increasing with increasing cooling rates, annealing times, and temperatures. For iPP/PA6 samples, the sPP−PA6 diblock copolymer had a sufficient stabilizing role on the interface to allow the observation of the iPP/PA6 epitaxy previously described, with a higher sensitivity of the degree of orientation to the annealing time than for sPP/PA6. The adhesive strength of macroscopic assemblies was also measured. The sPP−PA6 copolymer was able to mechanically reinforce the sPP/PA6 interface but not the iPP/PA6 one. The specific orientation of the polymers in the immediate vicinity of the interface is thus not sufficient to promote strong adhesion. The structure of the copolymer and its ability to entangle and probably cocrystallize with the matrix must also be considered.

Introduction

The association of two or more polymers in alloys, to obtain optimized products by combining their properties, is of great industrial importance. As most polymer pairs are immiscible, a compatibilizing agent, most often a diblock copolymer, is added to the blends to avoid phase separation and to prevent interfacial failure between the two phases.[1−3] In such blends, the characterization of the interface is of particular importance because of its influence on the final properties of the blend. In assemblies containing at least a semicrystalline polymer, the crystalline structure and orientation near the interface appear to be able to influence the properties of the assemblies. For instance, epitaxial crystallization has been shown to improve the mechanical properties (Young's modulus, fracture strength, etc.) of isotactic polypropylene/polyethylene and isotactic polypropylene/polybutadiene assemblies.[4−7] A relation has also been suggested between improved macroscopic adhesion and epitaxy in the case of a PP copolymer matrix toughened with EPR particles.[8]

A useful model system to investigate alloys made of two semicrystalline polymers is the interface between isotactic polypropylene (iPP) and polyamide 6 (PA6), and such assemblies have been particularly studied.[9−13] The interface is reinforced with iPP−PA6 diblock copolymers formed in situ by chemical reaction between the $-NH_2$ end of polyamide chains and modified polypropylene molecules bearing succinic anhydride groups. Boucher et al.[9,10] showed that the adhesion of such assemblies does not always follow Brown's model:[14] a significant increase of the efficiency of the copolymer molecules in enhancing the fracture toughness was observed for specific experimental conditions (high annealing temperature, high molecular weight of the PP block of the copolymer). This enhanced efficiency has never been observed for assemblies between glassy polymers and is then presumably related to the semicrystalline nature of the polymers. It has been shown that this increased efficiency was not related to the presence of the metastable β-phase of iPP near the interface of the samples.[10,11] Besides, no change in the microstructure of the sample could be detected within a micrometer of the interface.[11,12] This strongly suggests that the crystalline structure in the immediate vicinity of the interface plays a role in this strengthening effect. The crystalline structure of both iPP and PA6 in the very vicinity of the interface was thus characterized to try to understand its role in the mechanical reinforcement of the assemblies.[13] Thin films bilayers (about 110−120 nm) were characterized by X-ray diffraction experiments. An epitaxial crystallization of iPP on PA6 was observed, and it appeared to be sensitive to the annealing time, annealing temperature, and structure of the copolymer block in the same way as the adhesive strength. The exact links between adhesion and epitaxy and the importance of a cocrystallization between the iPP matrix and the PP block of the copolymer were not, however, fully elucidated.

To further investigate the role of the crystalline structure at the interface, we present here an investigation of assemblies of polyamide 6 with both isotactic and syndiotactic polypropylene (iPP and sPP), the interfaces being reinforced by sPP−PA6 diblock copolymers formed in situ. When the matrix is iPP, the PP block of the copolymer is not miscible and cannot crystallize with the PP matrix (iPP and sPP are known to be immiscible

† UMR 7125 CNRS-Collège de France.
‡ UMR 7615 CNRS-ESPCI.
§ Present address: Cray Valley, Research Center of Oise, Parc Alata, BP 22, 60 550 Verneuil en Halatte, France.
* To whom correspondence should be addressed. E-mail Liliane.leger@college-de-france.fr.

10.1021/ma040024g CCC: $27.50
Published on Web 08/06/2004

Table 1. Main Characteristics of the Products

product	M_n (kg/mol)	M_w/M_n	meso/racemic pentads (%)[a]	T_m (°C)[b]	crystalline fraction, χ[b] (%)	E (GPa)[c]	σ_y (MPa)[d]
PA6	18	1.9		221.0	~30	2.9[e] to 1.0[f]	65[e]
iPP	57	4.8	72/5	165.5	~45	1.25	27
sPP	48	4.0	0/76	117.0 and 129.3	~18	0.40	16
sPP_f	35.8	3.5	0/70	116.3 and 129.2	~14		

[a] Measured by ^{13}C NMR at 75 MHz, in 1,2,4-trichlorobenzene at 120 °C (7 wt % solution) with deuterated tetrachloroethane as an external lock. [b] Measured using Modulated DSC (T.A. Instruments 2820 modulated DSC). Data taken from the second heating scan (heating rate: 5 °C/min; modulation: 0.796 °C; period: 60s). χ was calculated using ΔH_m^0(sPP) = 230 J/g,[32] ΔH_m^0(PA6) = 230 J/g (*Handbook of Polymers*), and ΔH_m^0(iPP) = 207 J/g (*Handbook of Polymers*). [c] Measured by three-point bending test. [d] Measured by traction test. [e] Dry PA6. [f] Wet PA6.

in the melt[15−18]) on the contrary to the case where the matrix is sPP. Characterizations of both crystalline orientation and adhesion at the interface were carried out for both types of samples. The influence of annealing conditions and relative structure of PP matrix and copolymers on these properties will be discussed as well as the role of the observed epitaxy in the interface reinforcement of these systems.

Experimental Section

Materials. The polyamide 6 was Ultramid B3 from BASF, having an average of one $-NH_2$ end per chain. Isotactic polypropylene 3050MN1 from Appryl (Atofina) and a development grade syndiotactic polypropylene from Atofina were used for the other part of the assemblies. The PP matrix were mixed with 5 wt % of a succinic anhydride functionalized syndiotactic polypropylene (sPP_f) synthesized by Atofina with about one average anhydride group per chain. Such blends will be denoted iPP* and sPP* in the following. The copolymer formation occurs at the PP/PA6 interface during an annealing step above the PP melting temperature by reaction between the succinic anhydride group of the PP_f and the NH_2 end of the PA6. No appreciable reaction of the anhydride with an amide linkage could be detected in similar systems.[9]

The main physical properties of the products are listed in Table 1. We checked the miscibility of the sPP_f with the PP matrix by DSC experiments on 50/50 matrix/PP_f blends. These experiments showed that the sPP_f was able to cocrystallize with the sPP matrix. The DSC scans on iPP/sPP_f blends led to separate crystallization and melting peaks for i- and sPP, which confirmed the nonmiscibility of the products and their inability to cocrystallize.

Determination of the Crystalline Orientation of the Interface. Thin film bilayers were prepared by spin-coating solutions onto silicon wafers (Siltronix) as previously described.[13] The samples were subsequently annealed under vacuum to avoid oxidation. The wafers were placed on a hot surface, and the system was heated above the melting temperature of the PP matrix, the annealing temperature T_a being varied between 180 and 223 °C and the annealing time between 30 and 150 min. In the following, we call "annealing time" the time during which the temperature was larger than the melting temperature of the PP matrix. The iPP/PA6 samples were annealed with the following conditions: the plate was preheated at 140 °C; the films were heated at T_a during a given time and cooled to 125 °C with a cooling rate of about 1.25 °C/min before being quenched at room temperature. With such a cooling rate, the iPP crystallization peak recorded by DSC experiments presents a maximum at about 130 °C: the iPP film should then be completely crystallized before the final quench. Some sPP/PA6 samples were annealed with the same conditions as the iPP/PA6 samples. In this case the temperature reached before quenching (125 °C) was above the crystallization temperature of the sPP (about 80 °C), and the sPP crystallization occurred during the quench. Other samples were annealed with different conditions: the plate was preheated at 100 °C, the films were heated at T_a during a given time, cooled to 75 °C, and quenched at room temperature. The cooling rate around the sPP crystallization temperature is then about 0.5 °C/min, and the sPP should have completely crystallized before the quench.

Film thicknesses were measured by ellipsometry with a Sentech ellipsometer (λ = 632.8 nm) and calculated as the average of at least 10 measurements on each film surface. Thicknesses were systematically measured before annealing and were about 55 nm (±5%) for PA6 films and 60 nm (±10%) for PP films.

The crystalline orientation was determined by X-ray diffraction with the X-ray generator and detectors previously described.[13] The X-ray generator used in the diffraction experiments (Rigaku RU-200BEH) is a rotating anode operating at 40 kV and 25 mA with a copper target. A germanium (111) monochromator is used to select the Cu $K\alpha_1$ line (λ = 0.154 05 nm). The experiments were performed with incident angles α varying between 0.5° and 9° so that the diffraction configuration was varied between grazing incidence and $\theta/2\theta$ configuration (which allows the observation of the crystalline planes lying parallel to the surface). For iPP/PA6 samples, the detectors were centered in the position 2θ = 18° to detect the main diffraction peak of iPP and PA6. For sPP/PA6 samples, the detectors were centered either in the position 2θ = 15° (to better detect the main peaks of sPP) or in the position 2θ = 18° (to also detect the PA6 diffraction peaks). All data collected with the linear detector were scaled in time to be qualitatively and quantitatively compared.

In a thin polymer film, the crystalline orientation can be detected by X-ray diffraction as follows.[13] The intensity diffracted by the (hkl) planes is given by eq 1[19]

$$I_{hkl} \approx i_{hkl} p_{hkl} S \frac{e}{\sin \alpha} \quad (1)$$

i_{hkl} being the intensity diffracted by one crystallite, p_{hkl} the probability for (hkl) planes to be in diffraction position, S the cross section of the beam, and e the film thickness. Thus, the intensity diffracted by an isotropic thin film decreases when α increases, and only the most intense diffraction peaks should be observable because of the small quantity of material present in the sample. On the other hand, if a film is oriented so that (hkl) planes are parallel to the film surface, p_{hkl} is maximum for an incidence angle equal to the Bragg angle ($\alpha = \theta$). The intensity diffracted by these planes is then not expected to decrease so quickly with α, and a signal should be detectable in the $\theta/2\theta$ configuration. Besides, if a preferential orientation exists, one must observe a change in the diffraction pattern: the diffraction rings characteristic of the nonoriented polymer will be replaced by simple spots. In particular, crystalline planes parallel to the sample surface will give a spot in the plane of the incident beam. The better the orientation is, the smaller the lateral extension of the diffraction spots.

Fracture Toughness Measurements. The procedures of preparation and characterization of the macroscopic samples (G_c and Σ measurements) were similar to those developed by Boucher et al.[9,10] We briefly recall them here for the understanding of the present investigation.

sPP*, iPP*, and PA6 were compression molded in a Darragon press to obtain thick sheets. iPP* and sPP* were molded at 200 °C in 500 μm thick sheets; PA6 was processed at 250 °C to obtain plates with thickness between 0.8 and 2 mm. The

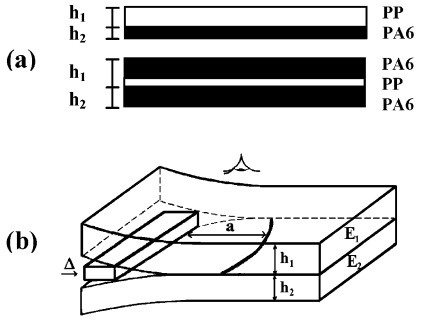

Figure 1. Fracture toughness measurements. (a) Samples geometries used for the ADCB test: simple joints (top) and sandwich geometry (bottom). (b) Principle of the ADCB test.

cooling rate was about 20−30 °C/min for all samples. The sheets were washed in an ultrasonic bath with ethanol and *n*-heptane before use. The PA6 sheets were dried at 80 °C under vacuum during 3 days and stored under vacuum in order to minimize the moisture sorption by PA6 and its resulting effects on the PA6 mechanical properties.

The assemblies were formed by clamping PA6 and PP* sheets together in airtight, Teflon-lined molds under controlled pressure. The thickness of each polymer side was adjusted by using an appropriate number of sheets. The molds were heated in a temperature-controlled furnace above the melting temperature of the polypropylene matrix. The annealing temperature was varied between 180 and 223 °C and the annealing time between 30 and 1000 min. The samples were cooled to room temperature by putting the molds on lead bricks at room temperature. The cooling rate was about 7−8 °C/min and about 2 °C/min around respectively the iPP and the sPP crystallization temperature. After cooling, the samples were stored in an atmosphere with controlled humidity and temperature (RH ∼ 58%, $T = 21$ °C) for at least 48 h before testing to control the PA6 moisture sorption and thus its Young's modulus (E_{PA6} is typically 1.6 GPa after storage). Two sample geometries were used (Figure 1a). For iPP/PA6 samples we used a simple joint geometry, the ratio $h_{PP}/(h_{PP} + h_{PA6})$ being kept in the range 0.57−0.70 determined by Boucher et al. to obtain consistent values of G_c.[9] The sPP being softer than the iPP and more able to plastically deform, sandwich geometry was chosen for the sPP/PA6 samples. This geometry was previously shown to be equivalent to the simple joint geometry.[10]

The fracture toughness (G_c) was measured using an asymmetric double cantilever beam (ADCB) test as shown in Figure 1b. A blade of thickness Δ was inserted between the two beams and pushed into the sample at a velocity of 90 μm/min (1.5 μm/s). As no dependence of G_c on the crack velocity was found in the range 0.3−300 μm/s,[9] we assumed that the measured value was equal to the critical energy release rate at zero velocity. The crack was observable through the PA6 beam, and images were recorded by use of a computer-driven video camera every 150 s after stabilization of the crack. About 40 images were recorded on each sample. The crack length a was then measured on the images using an image treatment software.

The following equations were used to evaluate G_c. They are based on the "beam on an elastic foundation" model proposed by Kanninen,[20] taking into account the elastic deformation of the materials ahead of the crack tip.

$$G_c = \frac{3}{8}\frac{\Delta^2}{a^4}\frac{E_1 {h_1}^3 E_2 {h_2}^3}{E_1 {h_1}^3 {\alpha_2}^2 + E_2 {h_2}^3 {\alpha_1}^2} \tag{2}$$

with

$$\alpha_i = \frac{1 + 3/\lambda_i a + 3/(\lambda_i a) + 3/2(\lambda_i a)^3}{1 + 1/\lambda_i a} \tag{3}$$

and

$$\lambda_i = \frac{\sqrt[4]{6}}{h_i} \tag{4}$$

In these equations, E_i and h_i are respectively the Young's modulus and the thickness of the side i of the sample. For the sandwich geometry, the equivalent modulus of the composite PP/PA6 beam was calculated. Taking into account the standard deviation of the measurement of the crack length, a, and the uncertainties on the physical constants and thickness of the beams, the estimated accuracy on G_c is about 10%.

XPS Determination of the Copolymer Surface Density. To determine the amount of copolymer formed at the interface of bulk samples, we used the method developed Boucher et al.[9] The PA6 beam of an unbroken part of ADCB samples on which G_c had been previously measured was selectively dissolved. This was achieved by use of three well-stirred formic acid baths (the total immersion time being at least 18 h). To be sure that no free PA6 was linked by hydrogen bonds to the copolymer chains, the samples were subsequently treated with trifluoroacetic anhydride in the gas phase. This step eliminated the amides of PA6 (hydrogen bond donors) by forming the corresponding imide. The residual free chains were removed by rinsing the samples with dichloromethane. The trifluoroacetyl groups on the grafted chains were then removed by hydrolyzation in desionized water. The samples were finally rinsed with *n*-heptane and absolute ethanol and dried under vacuum. They were then stored in glass flasks cleaned with a "piranha" mixture. They were analyzed within 10 days of preparation to minimize the oxidation of the PA6 layer.

The surface density of PA6 chains grafted onto PP* was determined by X-ray photoelectron spectroscopy (XPS): since PA6 contains nitrogen and PP does not, it is possible to quantify the thickness of a PA6 layer on a PP surface. The spectra were collected on a SSX-100 surface science spectrometer using a monochromatic source (Al $K\alpha_1$, $h\nu = 1486.6$ eV). The spectra were recorded at a takeoff angle of 35° between the sample and the detector and with an electron flood gun of 9 eV to dissipate charges in the sample. Survey scans between 0 and 1100 eV were first collected on each sample to check for surface contamination. The 1s spectra of carbon, nitrogen, and oxygen were then recorded on a clean area of the sample.

Only the C 1s and N 1s signals were used for the evaluation of Σ. As detailed previously,[9] the modeling was based on the assumption of the presence of a dense layer of PA6 of variable thickness at the surface. We also assumed that the succinic anhydride group was located at the end of the PP_f chains and that the grafted PA6 had a molecular weight distribution representative of that of the bulk. The surface density of copolymer chain is then evaluated using eq 5

$$\Sigma = -\frac{N_A \rho \lambda \sin\theta}{M_n} \ln\left(1 - \frac{I_N/I_C}{I_N^\infty/I_C^\infty}\right) \tag{5}$$

where N_A is Avogadro's number, ρ the mass density of PA6, M_n its number-average molar mass, λ the mean free path of N 1s photoelectrons, and θ the takeoff angle. The escape length of the photoelectrons, $\lambda \sin\theta$, was estimated to be 19 Å using an experimentally determined relationship for escape length through hydrocarbon layers.[21] I_C and I_N are the intensities of the carbon and nitrogen peaks on the analyzed sample surface, and I_C^∞ and I_N^∞ are the intensities of these peaks on a pure PA6 surface. The reproducibility of the Σ measurements was approximately ±10%.

Results

Crystalline Orientation at the Interface. Observations of the annealed samples under optical and AFM microscopy showed the effectiveness of the sPP_f−PA6 copolymer in stabilizing both the iPP/PA6 and the sPP/PA6 interfaces. While samples of pure iPP matrix

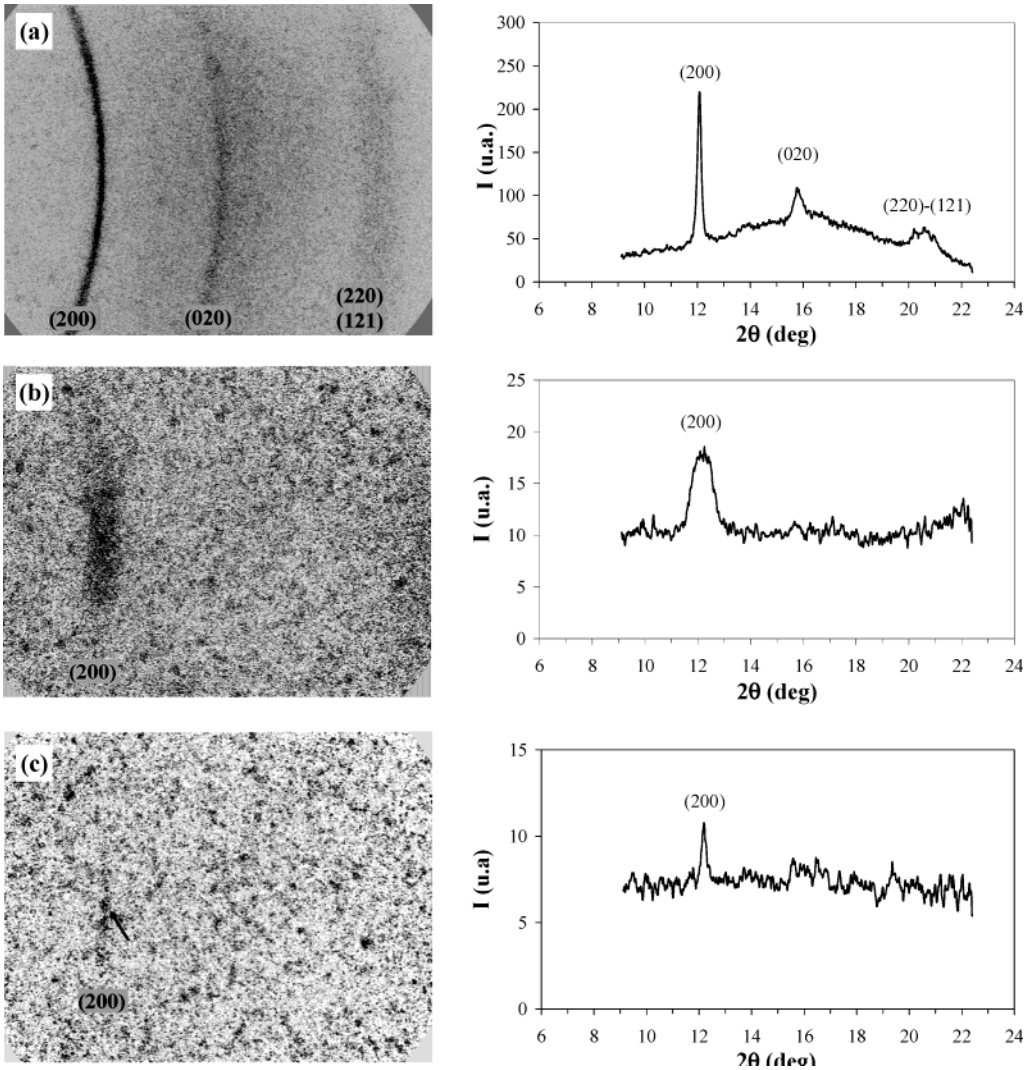

Figure 2. Diffraction spectra of syndiotactic polypropylene. Left: 2D diffraction spectra. Right: 1D diffraction spectra obtained by grouping together the points of a strip on the 2D spectra. (a, top) Bulk sPP, part of a compression-molded sheet. Spectrum acquired in the transmission mode. The diffraction pattern corresponds to the limit-disordered form I of sPP. (b, middle) sPP* film deposited on a PA6 film, annealed 102 min at 200 °C, and slowly cooled at 75 °C. Spectrum acquired in the reflection mode with an incidence angle of 0.5° and an exposition time of 24 h. The only visible diffraction ring corresponds to (200) planes, and only a part of the ring is present. The peak is enlarged because of the grazing incidence. (c, bottom) Spectrum acquired on the same sample with an incidence angle of 6° ($\theta/2\theta$ configuration for the (200) peak) and an exposition time of 24 h.

deposited on PA6 presented holes due to the dewetting of iPP even for low annealing time and temperatures,[13] no dewetting of the PP films was observed for all the samples containing sPP_f, whatever the annealing times and temperatures. Such observations show that the sPP_f−PA6 copolymer was formed at the interface and that it is able to prevent dewetting of the PP matrix on the PA6 substrate. This stabilizing effect occurs even when the PP block of the copolymer is not miscible with the PP matrix.

Figure 2 shows diffraction spectra obtained for bulk syndiotactic polypropylene (Figure 2a) and for a sPP* film deposited on a PA6 film (Figure 2b,c). The diffraction pattern of the bulk sPP is typical of the limit-disordered crystalline form I of sPP: it is characterized by the absence of the (211) diffraction ring for $2\theta = 18.8°$, visible in the diffraction pattern of the ordered crystalline form.[22] In the case of the sPP* film deposited on PA6, only the most intense diffraction ring of sPP, corresponding to the (200) planes, was observed. The diffraction intensity decreased with the incidence angle, but a signal was still observed in the $\theta/2\theta$ configuration (Figure 2c). Besides, only a part of that ring was visible. The diffraction spectra of sPP* films deposited on a bare silicon wafer gave the same diffraction peak, but the ring was complete, the intensity decreased more rapidly with α, and no signal was detected in the $\theta/2\theta$ configuration (data not shown). These observations demonstrate that the sPP film is oriented when deposited on a PA6 film. The PA6 induces a specific orientation of the sPP so that $(200)_{sPP-I}$ planes are parallel to the film surface.

Data showing how the annealing conditions influence the observed orientation are presented in Figures 3−5. The data were collected with the linear detector, and the intensities were scaled by the film thickness to be compared. As shown in Figure 3, increasing the cooling rate of the film led to an enhanced intensity for the $(200)_{sPP-I}$ planes, i.e., to a greater degree of orientation of the sPP. In the following, all the observations correspond to quenched sPP films. In Figure 4, the effect of the annealing temperature is reported. When T_a is increased above the melting temperature of PA6, the sPP orientation is much greater than for lower anneal-

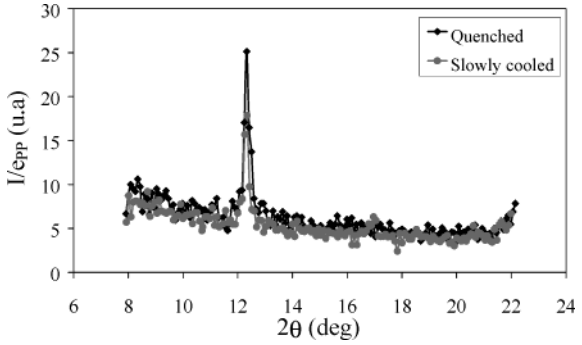

Figure 3. Influence of the cooling rate on sPP crystalline orientation. sPP* films deposited on PA6 and annealed 100 min at 200 °C. The linear detector is centered in the position $2\theta = 15°$, and the incidence angle is 7.5°.

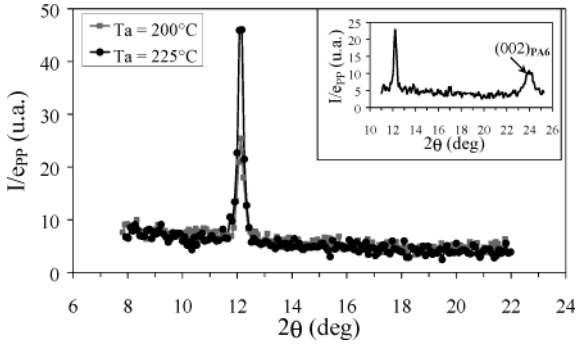

Figure 4. Influence of the annealing temperature T_a on sPP and PA6 crystalline orientation. sPP* films deposited on PA6, annealed 130 min and crystallized by quenching between 125 °C and room temperature. The linear detector is centered in the position $2\theta = 15°$, and the incidence angle α is 7.5°. Insert: diffraction spectrum of the sample annealed at 225 °C obtained with the detector centered in the position $2\theta = 18°$ and $\alpha = 9°$ to detect also the PA6 diffraction peaks.

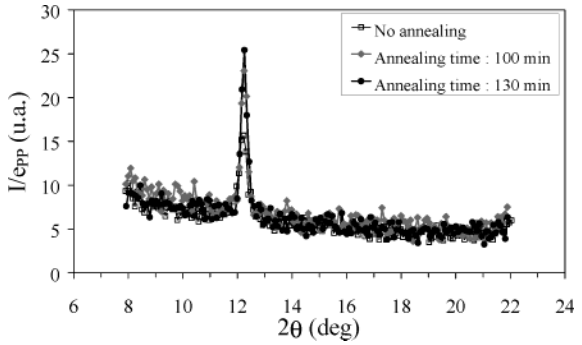

Figure 5. Influence of the annealing time on sPP crystalline orientation. sPP* films deposited on PA6, annealed at 200 °C, and crystallized by quenching between 125 °C and room temperature. The linear detector is centered in the position $2\theta = 15°$, and the incidence angle is 7.5°.

ing temperatures. Simultaneously, the diffraction peak of the $(002)_{PA6}$ planes appears at $2\theta = 24.0°$: the PA6 film reorganizes upon melting so that the $(002)_{PA6}$ planes become parallel to the film surface. The effect of the annealing time is reported in Figure 5. A nonannealed sample presents a weak but detectable sPP orientation. This orientation is greatly increased by the annealing, which allows the polymer melting and recrystallization, but the effect of a further increase of the annealing time is less pronounced.

Finally, we characterized the orientation of iPP/PA6 interfaces stabilized by sPP_f−PA6 copolymers. The diffraction spectra obtained (Figure 6) resemble those

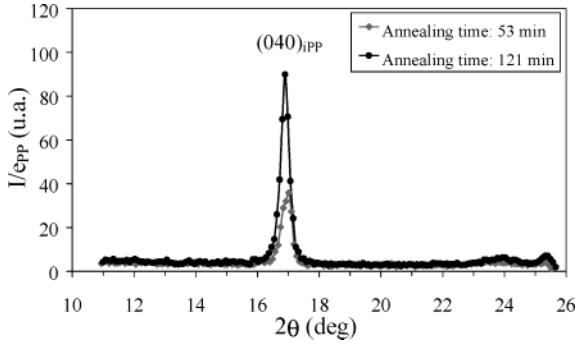

Figure 6. Influence of the annealing time on iPP crystalline orientation. iPP* films deposited on PA6 films and annealed at 200 °C. The linear detector is centered in the position $2\theta = 18°$, and the incidence angle is 9°.

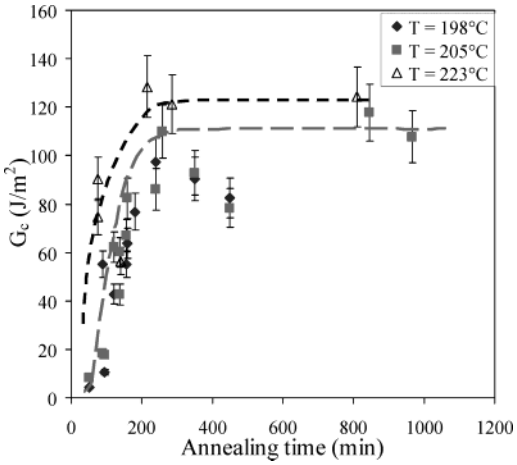

Figure 7. Kinetics of adhesion enhancement of the sPP/PA6 interface in the presence of sPP_f−PA6 copolymers for different annealing temperatures. The lines are guides for the eyes, aimed to extract over all tendencies. The rather large scatter in the data points comes from the small number of samples tested and to the intrinsic difficulty of forming these samples in a fully reproducible manner due to the rapid initial kinetics, which is quite sensitive to annealing time and temperature.

obtained on iPP/PA6 films stabilized by iPP_f−PA6 copolymers,[13] with an intense diffraction peak for the $(040)_{\alpha-iPP}$ planes at $2\theta = 16.9°$. This is characteristic of the epitaxy between iPP α phase and PA6 with iPP (040) planes parallel to the interface.[13] Nevertheless, the effect of the annealing time is much greater when using the sPP_f−PA6 copolymer than the iPP_f−PA6 ones. It is also greater than in the case of sPP/PA6 interfaces reinforced by the sPP_f−PA6 copolymer (cf. Figure 5).

Adhesion Measurements. The efficiency of the sPP_f−PA6 copolymer in stabilizing both sPP/PA6 and iPP/PA6 interfaces being established, its efficiency in reinforcing mechanically these interfaces was also tested. Figure 7 shows the kinetics of adhesion enhancement of the sPP/PA6 interface in the presence of the copolymer. A rapid enhancement of adhesion was observed for annealing times below 250 min, followed by a stabilization of the adhesion energy around 110 J/m^2. The shapes of the kinetics and the maximum adhesion energy reached are similar for annealing at 198, 205, and 223 °C, the latter being faster (the plateau being reached after about 200 min). The data recorded on the iPP/PA6 interface are displayed in Figure 8. The adhesion energies appear slightly larger than that of pure iPP on PA6 (which could not be measured due to spontaneous delamination of the assemblies and is thus

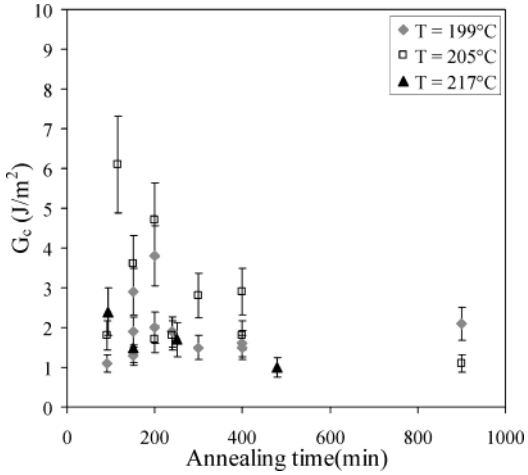

Figure 8. Adhesion enhancement of the iPP/PA6 interface in the presence of sPP_f−PA6 copolymers.

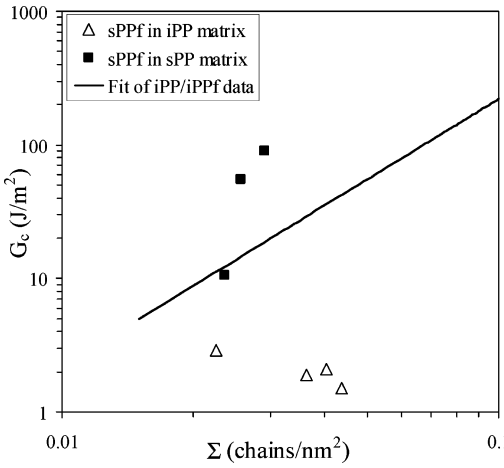

Figure 9. G_c as a function of the interfacial copolymer density Σ for the iPP/PA6 interface and sPP/PA6 interfaces in the presence of sPP_f−PA6 copolymers. The full line represents the best fit of G_c as a function of Σ^2, directly extracted from Boucher et al. data for iPP/PA6 samples in the presence of iPP/PA6 copolymer of low molecular weight.[9]

below 1 J/m^2) but are still very low (G_c < 6 J/m^2) whatever the annealing time and temperature. Besides, we noted that the fracture propagation was generally unstable in these samples.

The interfacial density of copolymers Σ of a few samples was also determined to evaluate the efficiency of sPP_f−PA6 copolymer in reinforcing PA6−iPP and PA6−sPP interfaces. The correlation between G_c and Σ measurements is shown in Figure 9. This figure confirms that the lack of mechanical strength of the iPP/sPP_f/PA6 samples was not due to a lack of copolymers at the interface but to their inefficiency to reinforce this interface, whatever the surface density. The low adhesion energies observed are compatible with a rupture mechanism by extraction of the copolymer chains. When used to reinforce the interface between sPP and PA6, the sPP_f−PA6 copolymers are however very efficient, and the adhesion energies measured are in the range observed for a rupture by crazing and copolymer chain scission (10−100 J/m^2). We also note that, for a given Σ, G_c is generally greater for the sPP/sPP_f/PA6 system than for the iPP/iPP_f/PA6 one. The exact rupture behavior is however difficult to establish since we were not able to measure Σ for a sufficient number of samples to be able to conclusively establish the exact shape of the $G_c(\Sigma)$ curve. Besides, the microstructure of the crack tip has not yet been observed, and we cannot confirm the effective presence of a craze.

Discussion

Crystalline Orientation of the Interface. The experiments presented above concerning the sPP/PA6 interface reveal an epitaxial crystallization of the syndiotactic polypropylene on the polyamide 6 substrate, with $(100)_{sPP}$ and $(001)_{PA6}$ planes (polymer chains planes[33]) tending to align parallel to each other. This is observed on a nonoriented PA6 substrate, which implies a strong interaction between the two polymers, a few PA6 lamellae with their (001) planes oriented parallel to the surface being sufficient to induce the epitaxy of sPP. The formation of the sPP_f−PA6 copolymer makes possible the observation of the epitaxy by preventing the dewetting of sPP on the PA6 substrate. This epitaxy can be related to previous results on epitaxial crystallization of syndiotactic polypropylene on polyethylene[23−26] and nylon-12,[27] both polymers crystallizing in their planar zigzag configuration. These epitaxial relationships are the result of the near parallelism of the aliphatic zigzag chains with the short pseudo *n*-pentane molecular segments of the sPP present in the $(100)_{sPP}$ planes. The axis of the polymer chains are then tilted at 37° to each other.[24] We suggest that the relationship between sPP and PA6 crystals is of the same type. The distance between two rows of pseudo *n*-pentane segments in $(100)_{sPP}$ planes is 4.47 Å, and the interchain distance in $(001)_{PA6}$ planes is 4.78 Å: the relatively good match between these two distances (6.9% discrepancy) allows an epitaxial growth of sPP on crystallized PA6. As a consequence, if a copolymer chain crystallizes on both sides of the interface, it will be, at least locally, parallel to the interface, as in the iPP/PA6 system.[13] Finally, the orientation induced by PA6 in sPP seems less important than in iPP films prepared in the same conditions. In particular, the signal recorded in the $\theta/2\theta$ configuration is less intense than in the grazing incidence geometry, contrary to the iPP/PA6 samples. This can be due to the weaker crystallinity of sPP compared to that of iPP (cf. Table 1) and/or to a weaker crystallographic relationship between sPP and PA6 than between iPP and PA6, the lattice mismatch being larger in the first case. In the iPP/ PA6 system, the epitaxy was attributed to the alignment of the PA6 chains on the methyl rows, these rows being separated by a distance of 0.505 nm.[13]

The preferential orientation of sPP chains on PA6 surfaces exists whatever the annealing conditions, but as seen in Figure 3, a rapid cooling leads to a greater degree of orientation. This is coherent with the results of Yan and Petermann showing that a rapid cooling favors a thick epitaxial layer in iPP/PE systems.[28,29] The same authors remarked that sPP/HDPE epitaxy is observed only when quenching the samples directly to room temperature.[26] This effect can be explained by the importance of the secondary nucleation process in the epitaxial crystallization. A rapid cooling favors the formation of numerous small secondary nucleation germs, leading to an important number of oriented lamellae and thus to a greater orientation. The epitaxy was also observed to be clearly greater when the films were annealed above the melting temperature of PA6, with a reorganization of both sPP and PA6 phases. The PA6 film recrystallizes with the low-energy (001) planes

parallel to the interface, as is the case in iPP/PA6 assemblies[13] or when PA6 is deposited on rubber surfaces.[30] The low surface energy of sPP melt favors the reorientation of the PA6 film. Because of this reorientation, the number of PA6 lamellae able to induce the sPP epitaxy becomes larger than in films annealed below the PA6 melting temperature, and the sPP orientation is greater (Figure 4). Increasing the annealing time has a much smaller effect on the reorientation (Figure 5). Increasing this time has a double effect: it increases the surface density of copolymer formed at the interface[9] and allows the reorganization of the PP phase in the melt. The small incidence of an increase of the annealing time on the orientation in sPP films shows that these factors have a relatively small influence on the epitaxy, the most important step being the recrystallization, as also shown by Figure 3.

For iPP/PA6 samples containing sPP_f, sPP_f−PA6 copolymers are formed and stabilize the interfaces, even if their PP block is not compatible with the matrix. The copolymers thus allow the observation of the epitaxy between iPP and PA6, but the PP block cannot crystallize with the matrix. The effect of the annealing time on the degree of orientation in these samples (Figure 6) is much greater than for the sPP/PA6 samples (Figure 5). This increase of epitaxy with annealing time in these assemblies is due neither to a reorganization of the PA6 film (the spectra presented were collected for samples annealed at 200 °C and show no sign of the PA6 diffraction peak at 24.0°) nor to the isotactic nature of the PP matrix, since the iPP/PA6 assemblies reinforced with iPP_f−PA6 copolymers show a much lower increase of epitaxy with the annealing time.[13] It is then probably related to the PP film reorganization. Long annealing times favor the iPP/sPP_f phase separation in the melt, probably helping the iPP film reorganization and thus improving its later crystallization.

Reinforcement of the Interfaces by the Copolymers. The sPP_f−PA6 copolymers have been shown to efficiently reinforce the sPP/PA6 interface, but not the iPP/PA6 one. This behavior has to be related to the miscibility of the PP matrix and the PP block of the copolymer. The miscibility between sPP_f and iPP being really poor, it leads to a lack of entanglements and of cocrystallization between the copolymer and the matrix and thus to the impossibility of an efficient stress transfer across the interface: the copolymer is simply extracted from the matrix during the fracture test. The sPP_f being miscible with the sPP, the sPP block of the copolymers can entangle and cocrystallize with the matrix chains, leading to an efficient reinforcement of the interface and to the possibility for a craze to develop at the crack tip. The exact fracture mechanism is however not certain at the present time, and further experiments of direct visualization of the deformed zones at the crack tip are needed to be more specific.

The effect of the annealing temperature on the fracture toughness was also tested. Contrary to the observation by Boucher et al.[10] of an increased efficiency of the copolymers by a factor of 4 for the high molecular weight iPP−PA6 block copolymers when iPP/PA6 samples were annealed above the melting temperature of PA6, no such enhanced adhesion was observed in the sPP/PA6 interfaces reinforced by sPP_f−PA6 copolymers. The adhesion energies remain in the same range for samples annealed below or above 221 °C. This behavior could be related either to the nature of the polypropylene matrix, the structure and mechanical properties of which are different from the one used by Boucher et al., or to the length of the copolymer chain that would not be sufficient to lead to an increase in efficiency vs adhesion in this system. In the absence of longer sPP_f chains we cannot discriminate at present between these two hypotheses.

Epitaxy/Adhesion Relationship. The important question is now to understand if the crystalline orientation of PP and PA6 near the interface plays a role in the mechanical reinforcement of the assemblies, as was shown in other systems.[4−8] In these systems, the authors explained the improvement of the properties of the assemblies by the fact that the epitaxially recrystallized lamellae of one polymer were able to bridge the soft amorphous regions in the substrate lamellar structure of the other polymer, thus enhancing the mechanical resistance of the weaker amorphous zones. Such an interpretation is not adequate to explain the observed behaviors in the studied PP/PA6 interfaces, where none of the polymers used are preoriented. Indeed, we observed a strong epitaxy at iPP/PA6 interfaces when sPP_f was used to stabilize and reinforce the interface while the corresponding adhesion was really poor. This implies that the epitaxy and the bridging of the softer zones by the epitaxially crystallized lamellae are not sufficient by themselves to promote a strong adhesion at the iPP/PA6 interface: the miscibility and cocrystallization of the PP block of the copolymer and PP matrix appear necessary for a good interfacial adhesion between iPP and PA6. In the sPP/sPP_f/PA6 system, where such a cocrystallization is possible, we observed both a clear orientation at the interface and a good adhesion. Yet the strong increase in the orientation degree observed for annealing temperatures above 221 °C was not correlated with a comparable adhesion enhancement as was the case in iPP/PA6 systems containing functionalized iPP chains of high molecular weight.[10,13] This implies that the degree of interfacial orientation does not play a direct role in the mechanical reinforcement of the sPP/PA6 interface either because of the nature of the interface or because of the structure of the copolymer. It is possible that the sPPf molecular weight is not sufficient to observe the same correlation between epitaxy and adhesion observed for high molecular weight PP_f in iPP/PA6 samples. Subsequent experiments implying longer sPP_f chains could help in understanding the coupling between interfacial orientation and adhesion at the interface.

Conclusion

The reinforcement of sPP/PA6 and iPP/PA6 interfaces by a sPP−PA6 copolymer has been investigated. The efficiency of this copolymer in stabilizing both interfaces and in preventing the dewetting of PP on PA6 has been established. The stabilization of the interface allowed the characterization of the crystalline orientation of the interface. These experiments clearly revealed an epitaxial crystallization of the sPP on the PA6 substrate. The corresponding degree of orientation is influenced by several parameters: cooling rate of the samples, annealing time, and temperature. Increasing these factors led to a more important degree of orientation of the polymer crystals in the immediate vicinity of the interface. The influence of annealing time and temperature was comparable to what has been previously observed on iPP/PA6 interfaces. In iPP/PA6 samples

reinforced by sPP/PA6 copolymers, we observed a greater influence of the annealing time on the degree of orientation, probably linked to a phase separation between the copolymer and the PP matrix.

Fracture toughness measurements on iPP/PA6 and sPP/PA6 samples were also carried out in order to try to understand the role played by the structure of the copolymer and the crystalline orientation at the PP/PA6 interfaces in the mechanical reinforcement of these assemblies. The results showed that the copolymer was able to efficiently reinforce the sPP/PA6 interface but not the iPP/PA6 one. This is directly related to the miscibility of the sPP_f with the PP matrix and its ability to develop or not entanglements and cocrystallization with the matrix.

The correlation between adhesion and orientation measurements showed that the presence of an interfacial orientation in the vicinity of the interface is not sufficient, alone, to promote adhesion at the PP/PA6 interfaces. A strong mechanical coupling (by entanglement or cocrystallization) is certainly a necessary condition for effective reinforcement. Furthermore, while the dependence of G_c on the copolymer molecular weight is not yet as clear as for glassy copolymers, it most probably affects the magnitude of the enhancement in fracture toughness of the interface.

Acknowledgment. The authors thank Atofina for financial support and for providing all the materials used in this study. We particularly thank Christian Quet (Atofina, Groupe de Recherches de Lacq) for access to the XPS apparatus and for his help in collecting the data. The ^{13}C NMR characterizations were kindly done by Françoise Lauprètre and Christine Sulpice-Gaillet from the Laboratoire de Recherche sur les Polymères (UMR CNRS 7581).

References and Notes

(1) Fayt, R.; Jérôme, R.; Teyssié, P. *J. Polym. Sci., Part B: Polym. Phys.* **1989**, *27*, 775−793.
(2) Brown, H. R. *Macromolecules* **1989**, *22*, 2859−2860.
(3) Creton, C.; Kramer, E. J.; Hadziioannou, G. *Macromolecules* **1991**, *24*, 1846−1853.
(4) Gross, B.; Petermann, J. *J. Mater. Sci.* **1984**, *19*, 105−112.
(5) Petermann, J. In *Polypropylene: Structure, Blends and Composites*; Karger-Kocsis, J., Ed.; Chapman & Hall: London, 1995; Vol. 1, pp 140−164.
(6) Petermann, J.; Xu, Y. *Colloids Polym. Sci.* **1991**, *269*, 455−459.
(7) Lee, H.; Schultz, J. M. *J. Mater. Sci.* **1988**, *23*, 4237−4243.
(8) Kestenbach, H.-J.; Loos, J.; Petermann, J. *Polym. Eng. Sci.* **1998**, *38*, 478−484.
(9) Boucher, E.; Folkers, J. P.; Hervet, H.; Léger, L.; Creton, C. *Macromolecules* **1996**, *29*, 774−782.
(10) Boucher, E.; Folkers, J. P.; Creton, C.; Hervet, H.; Léger, L. *Macromolecules* **1997**, *30*, 2102−2109.
(11) Kalb, F. PhD Thesis, Université Paris VI-Pierre et Marie Curie, 1998.
(12) Plummer, C. J. G.; Kausch, H.-H.; Creton, C.; Kalb, F.; Léger, L. *Macromolecules* **1998**, *31*, 6164−6176.
(13) Laurens, C.; Ober, R.; Creton, C.; Léger, L. *Macromolecules* **2001**, *34*, 2932−2936.
(14) Brown, H. R. *Macromolecules* **1991**, *24*, 2752−2756.
(15) Thomann, R.; Kressler, J.; Setz, S.; Wang, C.; Mülhaupt, R. *Polymer* **1996**, *37*, 2627−2634.
(16) Thomann, R.; Kressler, J.; Rudolf, B.; Mülhaupt, R. *Polymer* **1996**, *37*, 2635−2640.
(17) Maier, R.-d.; Thomann, R.; Kressler, J.; Mülhaupt, R.; Rudolf, B. *J. Polym. Sci., Part B: Polym. Phys.* **1997**, *35*, 1135−1144.
(18) Phillips, R. A. *J. Polym. Sci., Part B: Polym. Phys.* **2000**, *38*, 1947−1964.
(19) Guinier, A. *Théorie et technique de la radiocristallographie*; Dunod: Paris, 1964.
(20) Kanninen, M. F. *Int. J. Fract.* **1973**, *9*, 83−91.
(21) Laibinis, P. E.; Bain, C. D.; Whitesides, G. M. *J. Phys. Chem.* **1991**, *95*, 7017−7021.
(22) De Rosa, C.; Auriemma, F.; Vinti, V. *Macromolecules* **1997**, *30*, 4137−4146.
(23) Petermann, J.; Xu, Y.; Loos, J.; Yang, D. *Polymer* **1992**, *33*, 1096−1098.
(24) Schumacher, M.; Lovinger, A. J.; Agarwal, P.; Wittmann, J. C.; Lotz, B. *Macromolecules* **1994**, *27*, 6956−6962.
(25) Bonnet, M.; Loos, J.; Petermann, J. *Colloids Polym. Sci.* **1998**, *276*, 524−528.
(26) Yan, S.; Bonnet, M.; Petermann, J. *Polymer* **2000**, *41*, 1139−1145.
(27) Yan, S.; Petermann, J.; Yang, D. *Polymer* **1996**, *37*, 2681−2685.
(28) Yan, S.; Lin, J.; Yang, D.; Petermann, J. *J. Mater. Sci.* **1994**, *29*, 1773−1780.
(29) Yan, S.; Yang, D.; Petermann, J. *Polymer* **1998**, *39*, 4569−4578.
(30) Muratoglu, O. K.; Argon, A. S.; Cohen, R. E. *Polymer* **1995**, *36*, 2143-2152.
(31) Holmes, D. R.; Bunn, C. W.; Smith, D. J. *J. Polym. Sci.* **1955**, *17*, 139−177.
(32) Rodriguez-Arnold, J.; Zhang, A.; Cheng, S. Z. D.; Lovinger, A. J.; Hsieh, E. T.; Chu, P. P.; Johnson, T. W.; Honnell, K. G.; Geerts, R. G.; Palackal, J.; Hawley, G. R.; Welch, B. *Polymer* **1994**, *35*, 1884−1895.
(33) PP chain axis is **c**[22] (as usual for polymers), but PA6 chain axis is **b** for historical reasons.[31]

MA040024G